

## Multiplexed ionic current sensing with glass nanopores†

Cite this: *Lab Chip*, 2013, 13, 1859

Nicholas A. W. Bell,<sup>a</sup> Vivek V. Thacker,<sup>a</sup> Silvia Hernández-Ainsa,<sup>a</sup> Maria E. Fuentes-Perez,<sup>b</sup> Fernando Moreno-Herrero,<sup>b</sup> Tim Liedl<sup>c</sup> and Ulrich F. Keyser<sup>\*a</sup>

Received 14th January 2013,  
Accepted 12th March 2013

DOI: 10.1039/c3lc50069a

[www.rsc.org/loc](http://www.rsc.org/loc)

We report a method for simultaneous ionic current measurements of single molecules across up to 16 solid state nanopore channels. Each device, costing less than \$20, contains 16 glass nanopores made by laser assisted capillary pulling. We demonstrate simultaneous multichannel detection of double stranded DNA and trapping of DNA origami nanostructures to form hybrid nanopores.

### Introduction

Nanopores are showing great potential as a new technology for biophysics and molecular sensing. They are based on the simple resistive pulse principle that analytes can be detected by the exclusion of ions as they pass through a nanoscale channel.<sup>1</sup> Solid state nanopores made in insulating materials have been used for sensing a wide range of biomolecules.<sup>2–4</sup> Measurements are typically taken with a commercially available patch clamp amplifier (such as the Heka EPC 10 and Axon Axopatch 200B) measuring the ionic current across one nanopore at a time. Every nanopore experiment requires statistics on many single molecule translocations to collect meaningful data. Therefore multichannel systems present a clear advantage in terms of faster data collection. Integration of multiple channels into the same device also reduces the required concentration of analytes and enables the analysis of a single sample under different parameters such as applied voltage and nanopore size. Multiplexed recording of protein nanopores in lipid bilayers has previously been reported.<sup>5,6</sup>

Here we present, to our knowledge, the first example of multichannel ionic current detection of single molecules with solid state nanopores. Solid state nanopores have numerous advantages over protein nanopores such as robustness and tunability of pore size. Our system is based on glass nanopores which have previously been shown as alternatives to nanopores made in silicon nitride or graphene membranes.<sup>7,8</sup> This approach for nanopore device fabrication requires no clean room or ion beam facilities and has great advantages in terms

of manufacture time and cost per device. It also enables simultaneous optical imaging since the translocation of molecules is perpendicular to the objective axis.<sup>9</sup>

### Experimental details

#### Device fabrication

Quartz capillaries (Sutter) with inner diameter 0.2 mm and outer diameter 0.5 mm and containing a fused filament were used for all experiments. Capillaries were cleaned by sonication in acetone for 30 min followed by drying under a nitrogen gas stream and baking at 60 °C for at least 30 min to remove any residual acetone. Quartz capillaries were drawn down to a nanometre scale aperture with a laser assisted capillary puller (Sutter P-2000). A CO<sub>2</sub> laser is focussed onto the centre of a capillary to melt the quartz and forces are applied to the two ends of the capillary. The capillary tapers down and finally separates at the centre creating two glass nanopores with the pulling process lasting less than one second. The parameters used for pulling were Heat = 600, Fil = 0, Vel = 25, Del = 170, Pul = 225. It should be noted that the parameters for making nanopores can vary for different pipette pullers and therefore each must be calibrated with imaging of the size of the nanopores formed. Separately polydimethylsiloxane (PDMS) (Dow Corning) was cured in a 3D printed mold (Supplementary Fig. 1, ESI†) by mixing elastomer and curing agent in a ratio of 10 : 1 and baking at 60 °C for 24 h. Glass nanopores were placed in each of the 16 grooves contained in the PDMS and this was then plasma bonded to a glass microscope slide (Fig. 1a). To seal each channel a small amount of uncured PDMS was added to each groove and the device placed on a hot plate at 120 °C for five minutes to cure the PDMS. The device was then plasma cleaned for five minutes before adding solution to all reservoirs. In these experiments we used 10 mM Tris-HCl (pH = 8.0), 1 mM EDTA, 1 M KCl for double stranded DNA translocations (Fig. 1d) and 45 mM Tris-borate (pH = 8.3), 1 mM EDTA, 5 mM MgCl<sub>2</sub>, 1 M

<sup>a</sup>Cavendish Laboratory, J J Thomson Avenue, Cambridge, United Kingdom.

E-mail: [ufk20@cam.ac.uk](mailto:ufk20@cam.ac.uk); Fax: +44 (0)1223 337000; Tel: +44 (0)1223 337272

<sup>b</sup>Department of Macromolecular Structures, Centro Nacional de Biotecnología, Consejo Superior de Investigaciones Científicas, Madrid, Spain

<sup>c</sup>Center for NanoScience and Department of Physics, Ludwig-Maximilians-Universität München, Geschwister-Scholl-Platz 1, 80539 München, Germany

† Electronic supplementary information (ESI) available. See DOI: 10.1039/c3lc50069a

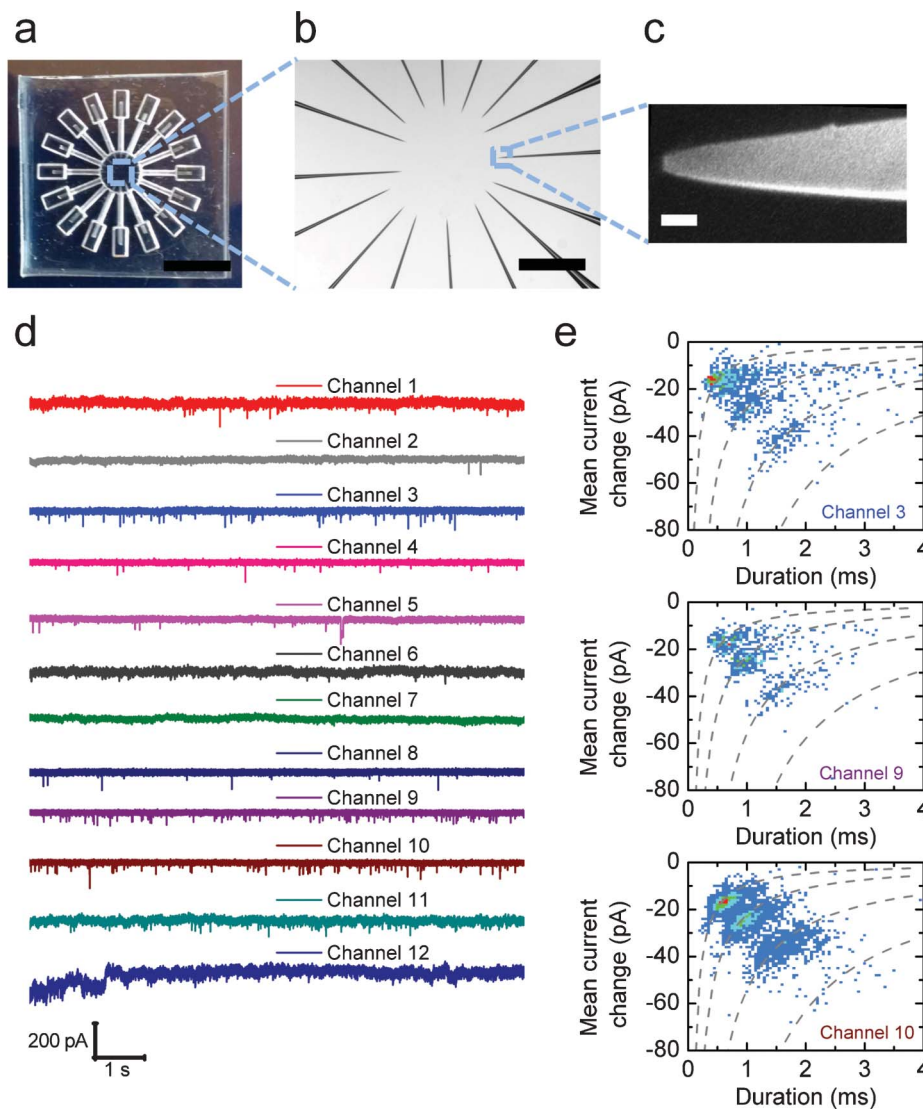


**Fig. 1** Simultaneous single molecule measurements of DNA with ionic current. (a) Macro image of 16 channel device. The nanopore orifices are all in the same central reservoir. Scale bar = 8 mm. (b) Optical image of central reservoir containing 16 glass nanopores formed at the tapered tip. Scale bar = 500  $\mu\text{m}$ . (c) SEM image of typical glass nanopore. Scale bar = 100 nm. (d) Simultaneous current traces of double stranded DNA translocation through 12 glass nanopores under 400 mV applied potential. (e) Statistical analysis of translocation events in (d) across three selected channels. Each graph shows a 2D frequency plot of the mean current change during a DNA translocation *versus* the duration of the translocation. Grey lines are hyperbolae fits for the four DNA lengths present in the sample. The number of events collected was as follows: Channel 3 = 1242 events, Channel 9 = 661 events, Channel 10 = 4463 events.

KCl for trapping of DNA origami (Fig. 2c). After adding solution, the device was placed under vacuum for two minutes to remove air bubbles. A single grounded Ag/AgCl electrode is placed in the central reservoir and 16 active Ag/AgCl electrodes connected in the outer ring of reservoirs.

#### Electrical measurements

We performed ionic current measurements with a 16 channel patch clamp Triton+ amplifier (Tecella). Each current signal was filtered at 10 kHz with the internal 6 pole Bessel filter of the amplifier. The current was recorded at 20 kHz sampling rate for each channel (the maximum sampling rate of the amplifier across all 16 channels) with 16 bit resolution using TecellaLab software. Current traces (Fig. 1d) were analyzed

with a custom written LabVIEW program (National Instruments).

#### Synthesis of DNA origami

The DNA origami was designed with the open source CaDNano v0.2 software. Synthesized oligos were ordered from Integrated DNA Technologies. The general method for preparation of DNA origami is reported elsewhere.<sup>10</sup> A 40  $\mu\text{L}$  solution with concentrations of 10 nM M13mp18 ssDNA scaffold (New England Biolabs), 100 nM of each staple, 14 mM  $\text{MgCl}_2$ , 10 mM Tris-HCl (pH = 8.0), 1 mM EDTA was made. This was placed in a thermocycler and annealed with a linear temperature decrease from 80  $^\circ\text{C}$  to 60  $^\circ\text{C}$  over 80 min followed by a linear temperature decrease from 60  $^\circ\text{C}$  to 25  $^\circ\text{C}$  over 1050

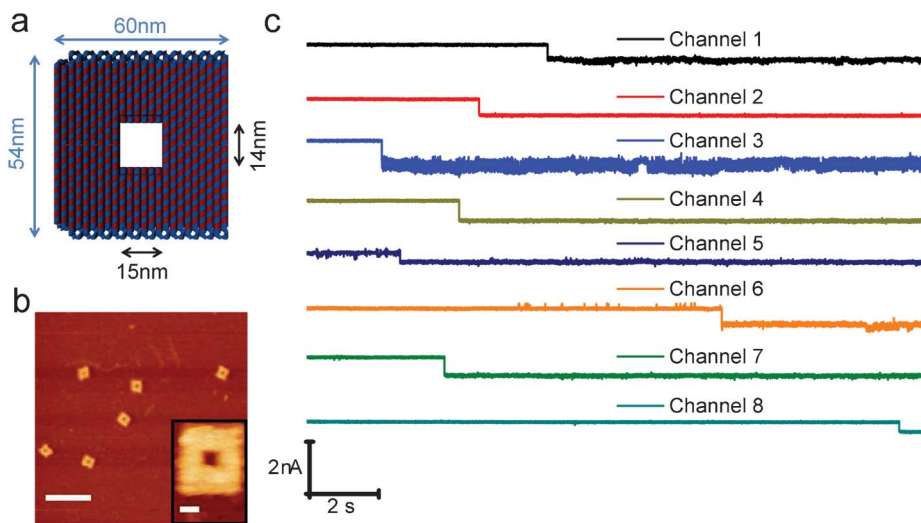


**Fig. 2** Multiplexed trapping of DNA nanostructures at a nanopore. (a) Schematic design of a DNA origami construct featuring a central 14 nm  $\times$  15 nm aperture. (b) Atomic force microscope images of assembled DNA origami structures deposited on mica. Scale bar = 200 nm. High resolution image inset. Scale bar = 20 nm. (c) Simultaneous current traces showing formation of hybrid DNA origami nanopores across multiple channels by trapping of DNA origami structures on glass nanopores. 600 mV is applied throughout and the 8 channels show a characteristic step decrease in current when one origami structure is trapped.

min. Excess staple strands were removed by centrifugation with 100 kDa cutoff Amicon filters (Millipore).

#### Atomic force microscope imaging

The overview image (Fig. 2b) was taken in tapping mode in air with Nanosensors PPP-NCLR tips (spring constant 48 N m<sup>-1</sup>). For the high resolution inset (Fig. 2b) measurements were performed in tapping mode with Olympus TR400-PSA tips (spring constant 0.08 N m<sup>-1</sup>) in buffer (10 mM Tris-HCl 8.0, 10 mM MgCl<sub>2</sub>, 2 mM NiCl<sub>2</sub>, 40 mM NaCl).

## Results and discussion

We have optimized the parameters of our laser capillary puller which creates nanopores with diameters less than 60 nm as determined by scanning electron microscopy (Fig. 1c). Glass nanopores (uncoated) were imaged with a Philips XL30 FEGSEM at 2 kV acceleration voltage. 10 Glass nanopores, made with the parameters listed in the methods, were imaged by SEM giving a distribution of outer diameters with a mean value of 42 nm and a standard deviation of 6 nm. The geometry of these nanopores, formed at the tip of a tapered capillary, enables simple integration to form a multichannel system with one small central reservoir (21  $\mu$ L volume) for the analyte to be measured (Fig. 1a and 1b).

We recorded simultaneous current traces of the translocation of double stranded DNA through a 16 channel glass nanopore device (Fig. 1d). The sample analysed is a linear double stranded DNA ladder (NoLimits, Fermentas) containing 2500, 5000, 10 000 and 20 000 base pair (bp) lengths at equal mass per unit volume concentrations. A bias of 400 mV is applied throughout. Data from only 12 channels is shown since two nanopores give no current due to obstruction with

large air bubbles and another two nanopores give current values above the dynamic range of the amplifier. All channels except 7 and 12 show clear downward spikes corresponding to translocations of DNA. The frequency of translocations varies between the channels which can be due to the different pore sizes and small variations in DNA concentration in the reservoir. Channels 7 and 12 have pronounced low frequency noise indicating poor wetting or non-specific clogging of the nanopore which can explain why we do not observe translocations.<sup>11</sup> Translocation event analysis of 8 min of simultaneously acquired current data from channels 3, 9 and 10 (Fig. 1e) shows that the 2500, 5000, 10 000 and 20 000 bp DNA lengths can be clearly distinguished by the characteristic inverse proportional dependence of event duration on mean current change.<sup>12</sup> A histogram analysis of the charge excluded during a single translocation also shows clear peaks corresponding to the DNA lengths (Supplementary Fig. 2, ESI†).

To further show the potential of our multichannel system we formed hybrid nanopores across multiple channels by combining DNA nanostructures with our glass nanopores. First experiments combining DNA origami with silicon nitride based solid state nanopores were recently published.<sup>13,14</sup> This approach has great promise for creating nanopores with controlled surface architecture and chemical functionality.<sup>15,16</sup> We designed a DNA origami structure two helices thick and 54 nm  $\times$  60 nm wide so that it would be too large to translocate through our glass nanopores and instead can be trapped at the tip to form a hybrid pore (Fig. 2a and 2b). The DNA origami has a central rectangular aperture 14 nm  $\times$  15 nm in size. These origami structures were added to the central sample reservoir of our device and a 600 mV potential applied (Fig. 2c). A sudden drop in current is observed upon trapping of a single DNA origami on 8 separate working nanopore

channels.<sup>13,14</sup> This method has the great advantage that although we have some variability in our glass nanopore diameter, the formation of the hybrid pore can fix the pore diameter according to the nanometre accurate design of the DNA origami.

## Conclusions

In summary, we present a simple and cost-effective method for multiple channel measurements of single molecules with solid state nanopores. Our fabrication of multichannel glass nanopore devices should extend the reach of nanopore techniques to researchers without access to clean room facilities and sophisticated transmission electron microscopes or ion beam equipment. Furthermore such multichannel experiments can greatly enhance statistical confidence in nanopore experiments.

## Acknowledgements

We thank Tecella for the loan of a Triton+ amplifier. N. A. W. B. was supported by a studentship from the EPSRC NanoDTC program. U. F. K. and S. H.-A. acknowledge support by an ERC starting grant. V. V. T. is grateful to the Cambridge Commonwealth Trust, the Jawaharlal Nehru Memorial Trust, and the Emmy Noether program of the Deutsche Forschungsgemeinschaft for support of his PhD position. T. L. acknowledges financial support from the DFG (SFB1032: Nanoagents) and the Nanosystems Initiative Munich (NIM). Work in the F. M.-H. laboratory was supported by a Starting Grant from the European Research Council (no. 206117) and a grant from the Spanish Ministry of Economy and Competitiveness (FIS2011-24638). M. E. F.-P. acknowledges

support by a contract from CSIC (contract number 200920I123).

## Notes and references

- 1 S. Bezrukov, *J. Membr. Biol.*, 2000, **174**, 1–13.
- 2 C. Dekker, *Nat. Nanotechnol.*, 2007, **2**, 209–15.
- 3 U. F. Keyser, *J. R. Soc. Interface*, 2011, **8**, 1369–1378.
- 4 M. Wanunu, *Phys. Life Rev.*, 2012, **9**, 125–58.
- 5 T. Osaki, H. Suzuki, B. Le Pioufle and S. Takeuchi, *Anal. Chem.*, 2009, **81**, 9866–70.
- 6 G. Baaken, N. Ankri, A.-K. Schuler, J. Rühle and J. C. Behrends, *ACS Nano*, 2011, **5**, 8080–8088.
- 7 L. J. Steinbock, O. Otto, C. Chimerele, J. Gornall and U. F. Keyser, *Nano Lett.*, 2010, **10**, 2493–2497.
- 8 L. J. Steinbock, O. Otto, D. R. Skarstam, S. Jahn, C. Chimerele, J. L. Gornall and U. F. Keyser, *J. Phys.: Condens. Matter*, 2010, **22**, 454113.
- 9 V. V. Thacker, S. Ghosal, S. Hernández-Ainsa, N. A. W. Bell and U. F. Keyser, *Appl. Phys. Lett.*, 2012, **101**, 223704.
- 10 S. M. Douglas, H. Dietz, T. Liedl, B. Högberg, F. Graf and W. M. Shih, *Nature*, 2009, **459**, 414–8.
- 11 R. M. M. Smeets, U. F. Keyser, N. H. Dekker and C. Dekker, *Proc. Natl. Acad. Sci. U. S. A.*, 2008, **105**, 417–21.
- 12 J. Li, M. Gershow, D. Stein, E. Brandin and J. Golovchenko, *Nat. Mater.*, 2003, **2**, 611–5.
- 13 N. A. W. Bell, C. R. Engst, M. Ablay, G. Divitini, C. Ducati, T. Liedl and U. F. Keyser, *Nano Lett.*, 2012, **12**, 512–7.
- 14 R. Wei, T. G. Martin, U. Rant and H. Dietz, *Angew. Chem., Int. Ed.*, 2012, **51**, 4864–7.
- 15 C. Martin, *Nat. Mater.*, 2012, **11**, 95.
- 16 M. Langecker, V. Arnaut, T. G. Martin, J. List, S. Renner, M. Mayer, H. Dietz and F. C. Simmel, *Science*, 2012, **338**, 932–936.